Published in final edited form as:
Brain Res. 2009 July 28; 1282: 142–155. doi:10.1016/j.brainres.2009.05.047.

MMP-9 gene silencing by a Quantum Dot-siRNA nanoplex delivery to maintain the integrity of the blood brain barrier

Adela Bonoiu[†,*], **Supriya D. Mahajan**[‡,*], **Ling Ye**[†], **Rajiv Kumar**[†], **Hong Ding**[†], **Ken-Tye Yong**[†], **Indrajit Roy**[†], **Ravikumar Aalinkeel**[‡], **Bindukumar Nair**[‡], **Jessica L Reynolds**[‡], **Donald E Sykes**[‡], **Marco A Imperiale**[‡], **Earl J. Bergey**[†], **Stanley A. Schwartz**[‡], and **Paras N. Prasad**[†,**]

[†]Institute for Lasers, Photonics and Biophotonics, University at Buffalo, The State University of New York, Buffalo, New York, 14260-3000

[‡]Department of Medicine, Division of Allergy, Immunology, and Rheumatology, University at Buffalo, The State University of New York, and Kaleida Health, Buffalo, New York, 14203

Abstract

The matrix-degrading metalloproteinases (MMPs), particularly MMP-9, are involved in the neuroinflammation processes leading to disrupting of the blood brain barrier (BBB), thereby exacerbating neurological diseases such as HIV-1 AIDS dementia and cerebral ischemia. Nanoparticles have been proposed to act as non-viral gene delivery vectors and have great potential for therapeutic applications in several disease states. In this study, we evaluated the specificity and efficiency of quantum dot (QD) complexed with MMP-9-siRNA (nanoplex) in downregulating the expression of MMP-9 gene in brain microvascular endothelial cells (BMVEC) that constitute the BBB. We hypothesize that silencing MMP-9 gene expression in BMVECs and other cells such as leukocytes may help prevent breakdown of the BBB and inhibit subsequent invasion of the central nervous system (CNS) by infected and inflammatory cells. Our results show that silencing of MMP-9 gene expression resulted in the upregulation of extracellular matrix (ECM) proteins like collagen I, IV, V and a decrease in endothelial permeability, as reflected by reduction of transendothelial resistance across the BBB in a well validated in-vitro BBB model. MMP-9 gene silencing also resulted in an increase in expression of the gene tissue inhibitor of metalloproteinase-1 (TIMP-1). This indicates the importance of a balance between the levels of MMP-9 and its natural inhibitor TIMP-1 in maintaining the basement membrane integrity. These studies promise the application of a novel nanoparticle based siRNA delivery system in modulating the MMP-9 activity in BMVECs and other MMP-9 producing cells. This will prevent neuroinflammation and maintain the integrity of the BBB.

Keywords

Nanotechnology; siRNA; Nanoplex; Blood Brain Barrier; Matrix metalloproteinases; MMP-9; Quantum Dot; CNS

**Corresponding author. E-mail: pnprasad@buffalo.edu.
*Equal contribution by both authors.

INTRODUCTION

The blood brain-barrier (BBB) plays a crucial role in homeostasis of the central nervous system (CNS), serving as the brain's protective shield against the entry of cells and soluble factors from blood to brain (Ellis et al., 2007). The BBB includes endothelial cells, astrocytes and pericytes, but their interactions in the formation or maintenance of the barrier have not been established (Teichberg, 2007). In neuroinflammatory conditions, such as multiple sclerosis, human immunodeficiency virus type-1 (HIV-1) encephalitis (HIVE), meningitis, cerebral ischemia, and brain tumors, the matrix-degrading metalloproteinases (MMP) play an important role in disrupting the BBB. MMPs are proteolytic enzymes that are instrumental in the turnover of the extracellular matrix (ECM), and are mediators of cell migration (Woessner Jr, 1991). Neurons, leukocytes, glial cells, and endothelial cells produce MMPs upon stimulation (Ellis et al., 2007; Paul et al., 1998; Gidday et al, 2005). Furthermore, it has been shown that viral infections of the brain enhance MMP expression several-fold (Sundstrom et al., 2001; Wu et al., 2000).

MMP-9 is also known to mediate the transmigration of inflammatory leukocytes across basement membranes, thus leading to proteolytic degradation of extracellular matrix (ECM) components. In addition to degrading the neurovascular matrix, MMP-9 promotes neuronal apoptosis by disrupting cell-matrix interactions that enhance the permeability of the BBB, thereby exacerbating neurological diseases such as HIVE. Studies with MMP-9 knockout mice have shown that diminished MMP-9 expression reduces BBB leakage (Asahi et al., 2001). In vitro studies using brain endothelial cell cultures activated with the proinflammatory cytokines, tumor necrosis factor-alpha (TNF-α) and interleukin-1beta (IL-1β), resulted in selective up-regulation of MMP-9 activity, whereas no significant changes were seen in the MMP-2 or TIMP-2 levels (Persidsky, 1997). This suggests that MMP-9 is a predominant MMP in neuroinflammatory processes leading to BBB leakage (Persidsky et al., 1997).

To invade the CNS, HIV-1 must migrate through the brain microvascular endothelial cells (BMVECs) that are a component of the BBB (Pulliam et al., 1997; Schmidtmayerova et al., 1997). The pathogenesis of HIVE is primarily attributed to infiltration of the CNS by HIV-infected mononuclear cells. HIVE often exhibits impairment of the BBB integrity (Persidsky, 1997; Persidsky, 2003; Annunziata, 2003; Langford et al., 2006).

The inhibition of MMP-9 activity via post-translational gene silencing using delivery of short interfering RNA (siRNA) molecules at BMVECs will have a significant impact on reducing the BBB permeability. However, a major hurdle limiting the use of this technology is the lack of methods to safely and efficiently deliver siRNA molecules to their target (Whitehead et al., 2009). In the free form, siRNA molecules have a very short half life in physiological conditions, owing to their vulnerability for degradation by endogenous nucleases. Therefore, they need nanoparticulate carriers (vectors) that will not only protect them from degradation in the biological milieu, but also steer them to desired cells/tissues as well as facilitate their cellular entry (Whitehead et al., 2009).

The use of semiconductor nanocrystals (NCs) or so-called quantum dots (QDs) as luminescence probes for numerous biological and biomedical applications has become an area of intense research over the last decade (Michalet et al., 2005; Prasad, 2003; Prasad, 2004).

QDs offer several advantages over organic dyes, including increased brightness, stability against photobleaching, broad absorption spectra, and a tunable and narrow emission spectrum (Prasad, 2004). As a result, they have demonstrated the potential to dramatically outperform conventional organic dyes in imaging of cellular and sub-cellular structures and in a variety of bioassays (Prasad, 2003; Prasad, 2004; Qian et al., 2007; Yong et al., 2007). The surface of the QDs can be easily functionalized to incorporate biologicals such as siRNAs, aptamers,

antibodies, peptides, and proteins (Michalet et al., 2005). Furthermore, the size of these nano-bioconjugates under physiological condition is typically less than 50 nm, making these QD-based nanoparticles ideal candidates for in vitro and in vivo studies and applications.

In this investigation, we evaluate the specificity and efficiency of QDs as nonviral gene nanocarriers for MMP-9 gene silencing in a primary brain endothelial cell line that is well known to be difficult to transfect. Additionally, we measured functional/physiological changes as a consequence of MMP-9 gene silencing in these BMVEC. We hypothesize that silencing of the MMP-9 gene expression in BMVEC will modulate the expression of ECM proteins like collagens I, III, IV, and V, and decrease endothelial permeability as reflected by reduction of transendothelial electrical resistance across the BMVEC monolayer. These studies will not only highlight the role of MMP-9 in the modulation of BBB permeability, but also validate a novel nanoparticle based system for efficient siRNA delivery.

RESULTS

Complex formation of siRNA with the QDs (nanoplexes)

Initially we determined the optimal conditions for the formation of QD-siRNA nanoplexes. For electrostatic complexation with the anionic siRNA molecules, cationically modified QDs were fabricated by coating a layer of the amine functionalized polymer polydiallyldimethylammonium chloride (PDDAC) on the surface of carboxyl terminated QDs. Two different QD: PDDAC ratios were used, represented as QD-15P and QD-30P, with the later containing twice the amount of the polymer than the former for the same amount of QDs (details provided in Materials and Methods). The physical and spectral characterization of the electrostatic complexes of QDs with siRNA was first determined using fluorescent labeled siRNA (siRNA$^{\mathbf{FAM}}$). The fluorescently labeled marker siRNA was designed for monitoring the uptake of siRNA by fluorescence microscopy or other fluorescence based technique, since it contained the fluorescein derivative FAM (5'-carboxyfluorescein) on the 5′ end.

To examine the binding efficiency of nanoplexes, we performed agarose gel electrophoresis using siRNA$^{\mathbf{FAM}}$ (green emitting) complexed with the two formulations of QDs (QD-15P and QD-30P, both red emitting). As shown in Figure 1A, free siRNA$^{\mathbf{FAM}}$ appeared as a leading band in the gel (lane 1). For the QD-only (QD-15P and QD-30P) bands, corresponding to lanes 2 and 4, respectively, all the fluorescence was observed in the wells, indicating that the QDs did not migrate into the gel. However, upon comparing the bands from the two nanoplexes, we found that while the green band for QD-15P-siRNA$^{\mathbf{FAM}}$ is slightly diminished (lane 3), it has completely disappeared in the case of QD-30P-siRNA$^{\mathbf{FAM}}$ (lane 5). This implies that the siRNA was partially and completely complexed with the QDs in the cases of QD-15P-siRNA$^{\mathbf{FAM}}$ and QD-30PsiRNA$^{\mathbf{FAM}}$, respectively. These results suggests that the QD-30P was more a efficient formulation of the two for siRNA complexation. It is worth noting though that the fluorescence from the siRNA$^{\mathbf{FAM}}$ was not apparent at the origin (well) of the gel owing to the overwhelming fluorescence signal emitted by the QDs. We have repeated this study with the same experimental set-up, except for using siRNA against MMP-9 (siRNA$^{\mathbf{MMP\text{-}9}}$). Since siRNA$^{\mathbf{MMP\text{-}9}}$ was non-fluorescent, this gel was stained with Ethidium Bromide (EtBr) for visualizing the siRNA (Figure 1B). The same outcome was observed as in Figure 1A, with the siRNA molecules partially (lane 3) and completely (lane 5) complexed by QD-15P and QD-30P, respectively. Data presented in Figure 1 is a representative gel from 3 separate experiments.

Size and spectral characterization

Transmission electron microscopy (TEM) images of QD-30P-siRNA$^{\mathbf{FAM}}$ nanoplexes showed that they remain as individual particles with a diameter of ~15–20 nm (Figure 2A). It can be

visualized from the TEM that siRNA complexation did not cause any aggregation of the QDs and this colloidal stability was observed for more than a month after complexation. Upon recording the emission spectra of the QD-30P-siRNA^{FAM} nanoplexes, as well as that of the 30P-QDs and siRNA^{FAM} individually, it was observed that the red emission (max ~620 nm) from the QDs increases at the cost of the green emission (max ~535 nm) from the siRNA^{FAM} upon complexation (Figure 2B). This was attributed to the process of fluorescence resonance energy transfer (FRET) from the siRNA^{FAM} (donor) to the QDs (acceptor), owing to the overlapping absorption spectra of the later with the emission peak of the former. This process of FRET is possible only when the two interactive species are in close physical proximity, in the range of a few nanometers from each other. Therefore, the observation of FRET in this case further substantiates complex formation between these two oppositely charged species.

Cellular uptake of fluorescent siRNA after QD-mediated delivery

Following the confirmation of the complexation of the siRNA^{FAM} with the QDs, the cellular uptake and intracellular distribution of the QD-15P-siRNA^{FAM} and QD-30P-siRNA^{FAM} nanoplexes were studied using confocal microscopy. Figure 2 shows emission from brain microvascular endothelial cells (BMVECs) treated with the nanoplexes, with the green emission coming from siRNA^{FAM}, red emission coming from the QDs, and the yellow emission is a result of an overlap of these two fluorescent species. However, in contrast, cells treated with free siRNA^{FAM} showed no emission at all. This demonstrates that the intracellular delivery of siRNA was mediated by the presence of QDs as carriers. Also, the superior siRNA complexation (Figure 1) and intracellular uptake (Figure 3) of the QD-30P-siRNA^{FAM} nanoplexes over that of the QD-15P-siRNA^{FAM} nanoplex suggests that the former nanoplex formulation was better suited over the later formulation for siRNA delivery. Therefore, in subsequent studies, only the QD-30P-siRNA^{FAM} or QD-30P-siRNA$^{MMP\text{-}9}$ formulation were used, which are hereafter referred to as QD-siRNA. Data presented in figure 2 and figure 3 are representative pictures from 3 separate experiments.

Effect of nanoplexes on cell viability

We evaluated the effect of QD complexed with siRNA, specific for the matrix metalloproteinase-9 (MMP-9) gene (siRNA$^{MMP\text{-}9}$), on the viability of BMVEC using the MTT assay (Promega, Madison, WI). We observed that BMVEC treated with QD-siRNA$^{MMP\text{-}9}$ nanoplexes remained >95% viable under all treatment conditions for up to 2 week (data not shown). This result demonstrates that the QD-mediated delivery of siRNA did not produce any appreciable cytotoxicity.

Efficiency of QD-siRNA$^{MMP\text{-}9}$ nanoplexes on knockdown of MMP-9 gene expression by BMVEC

After confirming the efficient QD-mediated cellular delivery of the marker siRNA^{FAM} (Figure 2) and its non-cytotoxicity, we investigated functional gene silencing efficiency using nanoplexes with siRNA$^{MMP\text{-}9}$. The efficiency of gene silencing was determined by measuring the percentage inhibition of the expression of the MMP-9 gene using quantitative, real-time PCR (Q-PCR). A fixed concentration of siRNA$^{MMP\text{-}9}$ (200 pmol) was complexed to QDs. Our results (Figure 4) show the decrease in MMP-9 expression by BMVEC treated with QD-siRNA$^{MMP\text{-}9}$ nanoplexes to be 78% [transcript accumulation index (TAI) = 0.22±0.03, p=0.0001], when compared to the negative control (Xtreme transfection reagent plus scrambled siRNA [200 pmol]) (TAI= 1.00±0.03). The positive control (Xtreme-siRNA$^{MMP\text{-}9}$ [200pmol] complex) also showed a significant inhibition of MMP-9 gene expression (52% suppression; TAI= 0.48±0.13, p=0.019), although lower than that observed using the nanoplexes at 48 hours post-transfection. Thus, our results showed that the QD-siRNA nanoplexes were superior to

the commercially available transfection agent in terms of increased transfection efficiency. Additionally, the shelf life of the QDs was excellent as compared to the commercial transfection agent and these QDs were stable at RT for several weeks and could be used for complexation with siRNA, up to 4 weeks post synthesis.

Decreased MMP-9 enzyme activity in BMVEC transfected with QD-siRNA^{MMP-9} nanoplexes

In addition to the significant decreases in MMP-9 gene expression observed in BMVEC transfected with QD–siRNA^{MMP-9} nanoplexes, we also evaluated the biological activity of MMP-9 in lysates of transfected BMVECs. Zymography was used to determine changes in the MMP-9 protein synthesis and/or activity. Our results (Figure 5) show that the MMP-9 activity in BMVECs treated with QD-siRNA^{MMP-9} nanoplexes decreased by 56% ($p<0.01$), when compared to that of the negative control. The positive control gave a 21% inhibition of the MMP-9 activity as compared to the negative control. These data (Figure 4 and Figure 5) showed that the transfection of BMVECs with QD-siRNA^{MMP-9} resulted in both a significant decrease in the expression of the MMP-9 gene and a corresponding decrease in the biological activity of MMP-9. Moreover QD-siRNA^{MMP-9} produced a greater suppression of the MMP-9 activity than that obtained using the commercially available transfection agent, Xtreme. Thus, QD-siRNA can be considered to be highly effective agent for gene silencing.

Effect of MMP-9 gene silencing on the expression of TIMP-1 and EMMPRIN genes

MMPs are selectively inhibited by tissue inhibitors of metalloproteinases (TIMPs). TIMP-1 binds to both the active and precursor form of MMP-9, and inhibits its enzymatic activity. In neuroinflammatory conditions, there is a reciprocal regulation of the expression of levels of MMP-9, which is elevated, and TIMP-1, which is decreased, in BMVECs. MMP activation also results in increased levels of the extracellular matrix metalloproteinase inducer (EMMPRIN). EMMPRIN is a 57kD transmembrane glycoprotein that can stimulate production of various MMPs (Foda, 2001). EMMPRIN is believed to have a role in physiological tissue remodeling by inducing stromal MMPs. However, in the BBB, EMMPRIN could consequently result in damage to the basal lamina, thereby disrupting the BBB. When BMVEC were treated with QD-siRNA^{MMP-9} nanoplexes, we observed a significant increase in the TIMP-1 gene expression ($p<0.01$) compared to BMVECs transfected with the scrambled control (Figure 6). However, no significant change was observed in the EMMPRIN gene expression.

Effect of MMP-9 gene silencing on MMP-9 and TIMP-1 protein expression

Using immunofluorescent microscopy, we evaluated the effect of MMP-9 gene silencing on MMP-9 and TIMP-1 protein synthesis. Our results show a decrease in the MMP-9 protein expression in BMVECs treated with QD-siRNA^{MMP-9} (Figure 7A and 7B). Further, an increase in the TIMP-1 expression in the QD-siRNA^{MMP-9} transfected cells was observed (Figure 7C and 7D).

In addition to immunofluorescent staining, we quantified the protein levels of MMP-9 and TIMP-1 using an ELISA kit. Cell culture supernatants from 4 separate experiments, where BMVEC cells were transfected with the transfection agent Xtreme complexed with siRNA against MMP-9 (Xi-siRNA^{MMP-9}) and QD conjugated siRNA nanoplexes, (15P) QD-siRNA^{MMP-9} and (30P) QD-siRNA^{MMP-9} respectively were harvested and the MMP-9 and TIMP-1 protein levels were quantified using commercially available ELISA kits (R&D systems). Our results (Figure 8) show that MMP-9 protein levels (ng/ml) for cells treated with Xi-siRNA^{MMP-9}, (15P) QD-siRNA^{MMP-9} and (30P) QD-siRNA^{MMP-9} were 10.01±1.26 ($p=0.007$), 6.40±1.56 ($p=0.004$), and 4.24±1.36 ($p=0.005$), respectively and were significantly lower than the untreated control (14.42±1.99 ng/ml). On the other hand, the TIMP-1 protein levels (ng/ml) for cells treated with Xi-siRNA^{MMP-9}, (15P) QD-siRNA^{MMP-9} and (30P) QD-siRNA^{MMP-9} were 3.10±1.61 ($p=0.03$), 5.84±1.90 ($p=0.007$), and 8.07±1.88 ($p=0.003$),

respectively and were significantly higher than the untransfected control (0.35±0.25 ng/ml). The significant modulation of the expression of MMP-9 and TIMP-1 protein as a consequence of MMP-9 gene silencing in BMVEC demonstrates that there is a dynamic balance between the expressions of these inter-related genes and proteins.

Effect of MMP-9 silencing on the gene and protein expression of Collagens Iα1, III, IV and V by BMVEC

Collagens are the major component of the basal lamina which is essential for maintenance of the endothelial permeability barrier. A BBB breakdown in neuroinflammation is secondary to degradation of the basement membrane collagen mediated by MMPs. MMPs rigorously regulate microvascular permeability and basement membrane remodeling during an early inflammatory response (Foda and Zucker, 2001). Therefore, we hypothesize that gene silencing of MMP-9 also can modulate the expression of various members of the collagenase family. We evaluated the effect of silencing MMP-9 gene expression in BMVEC by QD-siRNA$^{\mathbf{MMP\text{-}9}}$ nanoplexes on the expression of the collagen Iα1, collagen III, collagen IV and collagen V genes. Our results (Figure 9) show that BMVECs transfected with QD-siRNA$^{\mathbf{MMP\text{-}9}}$ show a significant increases in the expression of collagen Iα1 ($p<0.001$), collagen IV ($p<0.01$) and collagen V ($p<0.05$) genes, but no change in collagen III gene expression, when compared to the negative control consisting of QDs conjugated to scrambled siRNA.

Protein expression studies using western blot analysis (Figure 10A & B) corroborated the finding of our gene expression studies. Cell lysates from BMVEC cells transfected with the transfection agent Xtreme complexed with scrambled siRNA (Xi-siRNA $^{\text{scrambled}}$), siRNA against MMP-9 (Xi-siRNA$^{\mathbf{MMP\text{-}9}}$), and QD conjugated siRNA nanoplexes, (15P) QD-siRNA$^{\mathbf{MMP\text{-}9}}$ and (30P) QD-siRNA$^{\mathbf{MMP\text{-}9}}$ respectively were used for western blot analysis of Collagens Iα1, III, IV and V. Our results (Figure 10A & B) showed that Collagens Iα1, III and V protein levels for cells treated with (15P) QD-siRNA$^{\mathbf{MMP\text{-}9}}$ (Lane 4) and (30P) QD-siRNA$^{\mathbf{MMP\text{-}9}}$ (Lane 5) were significantly higher than the untransfected control (Lane 1) while the Collagen IV protein levels were significantly lower in cells transfected with (15P) QD-siRNA$^{\mathbf{MMP\text{-}9}}$ and (30P) QD-siRNA$^{\mathbf{MMP\text{-}9}}$. The Collagen Iα1, III and V protein expression was increased 77% ($p<0.01$) and 135% ($p<0.01$); 121% ($p<0.01$) and 152% ($p<0.01$); and 121% ($p<0.01$) and 106% ($p<0.01$) respectively in (15P) QD-siRNA$^{\mathbf{MMP\text{-}9}}$ and (30P) QD-siRNA$^{\mathbf{MMP\text{-}9}}$ MMP-9 transfected cells as compared to the untransfected control. On the other hand, the Collagen IV protein expression was decreased 96% ($p<0.01$) and 98% ($p<0.01$) respectively in (15P) QD-siRNA$^{\mathbf{MMP\text{-}9}}$ and (30P) QD-siRNA$^{\mathbf{MMP\text{-}9}}$ MMP-9 transfected cells as compared to the untransfected control. These results indicate that silencing of the MMP-9 gene expression in BMVEC with QD-siRNA$^{\mathbf{MMP\text{-}9}}$ induces a coordinated modulation of the gene and protein expression of various collagens, all of which are involved in tissue remodeling secondary to inflammation.

Effect of MMP-9 gene silencing on the functional integrity of an in-vitro BBB model

Neuroinflammation is associated with an increase in the MMP-9 activity and a subsequent breakdown of the BBB, resulting in its increased permeability. This facilitates the transmigration of leukocytes across the BBB into the CNS. In the current study, we used a well validated, in-vitro BBB model to demonstrate the effect of MMP-9 gene suppression on the integrity of the BBB as measured by transendothelial electrical resistance (TEER). The inhibition of MMP-9 gene expression by transfection of BMVEC with QD-siRNA$^{\mathbf{MMP\text{-}9}}$ may prevent damage to the BBB, as reflected by an increase in TEER in our BBB model. Figure 11 shows a 30% (259±10.61 Ω/cm^2) increase in TEER in culture wells 48 hr after transfection of BMVEC with QD-siRNA$^{\mathbf{MMP\text{-}9}}$, compared to the untransfected controls. In our model, BBB formation usually takes 5–6 days and a TEER value of ~250 Ω/cm^2 indicates an intact BBB. There was no significant difference in TEER measurements between the untransfected

controls (189±4.12 Ω/cm^2) and the Xtreme transfected, scrambled siRNA negative controls (202±14.14 Ω/cm^2). These data suggest that silencing of the MMP-9 gene expression in BMVEC may be useful for the treatment of a variety of neuroinflammatory states that may compromise the integrity of the BBB.

DISCUSSION

The pathogenesis of HIVE (Persidsky, 1997; Persidsky, 2003) is associated in part with BBB breakdown and infiltration of HIV infected mononuclear cells into the CNS. Increased permeability of the BBB is an early and critical event that often precedes symptoms of HIVE. MMPs are a family of zymogen proteases, which under normal physiological conditions are involved in the degradation and remodeling of the extracellular matrix. MMPs degrade the basal lamina proteins, fibronectin, laminin and collagens, and also modulate the tight junction proteins (TJPs). Subsequent proteolysis of the microvascular basal lamina thus causes a breakdown of the BBB (Abbott, 2005; Abbott, 2004; Paul et al., 1998). Although neurons produce MMP-9, within the CNS, leukocytes are the major cellular source of MMP-9, which in turn facilitates further leukocyte recruitment (Gidday et al., 2005). The passage of leukocytes through basement membranes involves proteolytic degradation of extracellular matrix (ECM) components. Matrix metalloproteinase (MMP)-9 mediates transmigration of inflammatory leukocytes across basement membranes and this has significant relevance in several pathological conditions such as cancer, allergic asthma and neurological disorders. Localized tissue MMP-9 levels also play an important role in cell trafficking. MMP-9 gene deletion in endothelial cells will cause a reduction in BBB disruption by modulation of tight junction proteins and also reduce leukocyte trafficking across the BBB.

A new therapeutic intervention, silencing MMP-9 gene expression in cells that constitute the BBB, may be useful in neuroinflammatory conditions such as HIVE, to prevent breakdown of the BBB and inhibit subsequent invasion of the CNS by HIV infected leukocytes. Several strategies for delivery of siRNA using nanoparticles have been investigated, including encapsulation/complexation of siRNA in lipid and polymer based nanomaterials. However, the larger size (diameter above 200 nm) and potential antigenicity of such materials have limited the progress of siRNA technology into the clinic. We have synthesized ultrasmall QD-bioconjugates (diameter 15–20 nm, Figure 2) which are water-dispersible, photostable, and easily form stable electrostatic complexes with siRNA molecules. The efficient complexation of siRNA with the QDs and their cellular delivery was confirmed using fluorescently labeled siRNA (Figure 1 and Figure 2). Additionally, our nanoplexes manifested no toxic effects on cells and >95 % viability was observed (data not shown).

Using siRNA against MMP-9, the QD mediated gene silencing efficiency of almost 80% was obtained in BMVECs (Figure 4). Zymography, immunofluorecence studies and protein quantification using ELISA methodologies also correlate this significant decrease in MMP-9 expression in BMVECs mediated by QD-siRNA$^{\mathbf{MMP\text{-}9}}$ (Figure 5–Figure 8, respectively). We observed that MMP-9 gene silencing in BMVEC by QD-siRNA$^{\mathbf{MMP\text{-}9}}$ also affected the expression of other genes. TIMP-1 expression was significantly up-regulated in BMVEC by QD-siRNA$^{\mathbf{MMP\text{-}9}}$ (Figure 7 and Figure 8). Under physiological conditions the activity of MMP-9 is regulated on several levels, including gene transcription, activation of inactive precursors, and modulation of TIMPs. A down regulation in MMP-9 activity was observed in BMVEC in which MMP-9 gene expression was silenced using the nanoplexes. However a similar magnitude of decrease in MMP-2 activity was not observed in these cells this may be attributed to the fact that despite the functional similarities of MMP-2 and MMP-9, the promoters for MMP-2 and -9 are structurally distinct (Bergman et al., 2003). The activation of MMPs can occur within the cell, at the cell surface or extracellularly by oxidative stress (Wang et al., 2002), and under conditions of oxidative stress the full length form of the MMP-2 may

also be proteolytically active. In the current experimental paradigm, cells were not undergoing any oxidative stress, and therefore we did not see intense proteolytic activation of MMP-2.

MMP-9 is secreted as pro-MMP-9, and requires activation by proteolytic enzymes for its catalytic function. The molar ratio of endogenous MMP-9 to TIMP-1 dictates whether pro-MMP-9 activation can progress. When the MMP-9/TIMP-1 ratio exceeds 1.0, MMP-9 activation occurs through a protease cascade involving plasmin and stromelysin 1 (MMP-3) (Ramos-DeSimone 1998). Thus there is a dynamic balance between the expression of MMPs and TIMPs. Any perturbation of this equilibrium, such as silencing of MMP-9 expression may secondarily affect TIMP-1 expression, as we observed (Figure 6, Figure 7 and Figure 8) particularly since it is believed that the activity of the MMPs may be modulated by the endogenous TIMPs.

Collagens are the principal substrate of MMPs. The sum balance of collagen deposition is a function of both their synthesis and degradation. We observed that silencing MMP-9 gene expression in BMVEC also caused reciprocal increases in the expression of various collagens, notably Iα1, IV and V (Figure 9 and Figure 10). MMPs are best known for their actions in ECM remodelling. MMPs degrade collagens I, III, IV and V which are their natural substrates. All of these genes are interrelated and are involved in remodeling of the ECM. We noted a significant increase in the gene and protein expression of collagens Iα1 and V, and although we did not observe a significant increase in Collagen III gene expression, a significant increase in the protein levels of Collagen III was observed in the MMP-9 transfected cells, further both gene and protein expression levels of Collagen IV were significantly decreased in MMP-9 transfected cells. Collagen Iα1 and Collagen III are both not substrates for MMP-9, while Collagen IV is a MMP-9 substrates. Collagen type IV represents ~50% of all basement membrane proteins, and has the capacity to self-assemble into organized networks. Unlike fibrillar collagens of types I, II, III, and V, type IV collagen is found to be crucial for basement membrane stability and assembly (Timpl, R et al., 1981). Since, Collagen type IV is a key MMP-9 substrate, it is not surprising that a suppression of MMP-9 gene expression resulted in a significant decrease in Collagen type IV expression. The other collagen types I, III, and V that we quantified in the study, were increased in BMVEC in which MMP-9 expression was inhibited using the siRNA nanoplexes. This may be arrtibuted to the fact that inhibition of MMP activity is associated with less deposition of fibrotic tissue, while the total matrix collagen content is a function of both synthesis and degradation, the degraded products of matrix proteins may serve as stimulators for collagen synthesis (Maquart F et al 1988;Li Y et al 2000). The changes in gene and protein expression of these family of Collagens observed, may be secondary to changes in a well orchestrated, complex, dynamic, network of inter-related genes and proteins involved in the recurring changes in the ECM that occur in both healthy and diseased states.

EMMPRIN is involved in the breakdown of the BBB by inducing nuclear factor (NF)-κB that, in turn, increases the expression of the proinflammatory cytokines, IL-6 and TNF-α(Schmidt et al., 2008). NF-κB binding by inflammatory cytokines is necessary for the upregulation of MMP-9. The MMP-9 promoter has an upstream nuclear NF-κB site that is crucial to its activity (Bond et al., 1998). However, no changes in the gene expression of EMMPRIN were observed in BMVEC treated with QD-siRNA$^{\mathbf{MMP\text{-}9}}$. This is not a surprising finding, as no stimuli for inflammation were used in our system, thus no effects on EMMPRIN expression were anticipated. Moreover, the lack of an effect on EMMPRIN expression serves as a good, negative control for the effects of QD-siRNA$^{\mathbf{MMP\text{-}9}}$ on the gene expression of TIMP-1 and the collagens. Thus, the up-regulation of TIMP-1 and collagen gene expression is highly selective.

This suggests that there is a balance in the expression of various genes involved in tissue remodeling, and any changes in the expression one alters the homeostasis between them,

resulting in concomitant changes in the expression of other functionally related genes. Our gene, protein expression and immunofluorescence studies also show a significant increase in the TIMP-1 expression in BMVEC transfected with QD-siRNA$^{\mathbf{MMP\text{-}9}}$. Levels of TIMP-1 in BMVEC are decreased under neuroinflammatory conditions in which the MMP-9 levels are increased. An increase in the TIMP-1 expression in BMVEC transfected with QD-siRNA$^{\mathbf{MMP\text{-}9}}$ is likely due to a response to an alteration in the normal MMP/TIMP ratio. This confirms the importance of the balance between the levels of MMP-9 and its natural inhibitor TIMP-1 in maintaining the basement membrane integrity. Although, the TIMPs in general do not demonstrate specificity for any particular MMP, TIMP-2 has been shown to have some degree of preference for MMP-2 and TIMP-1 for MMP-9 (Brew et al., 2000; Goldberg et al., 1992). Thus, MMP-9 modulation resulted in a significant increase in TIMP-1 gene and protein expression, and while we did not measure the levels of TIMP-2, we can speculate that the levels of TIMP-2 may not have changed significantly in these cells, thereby not altering the MMP-2 activity significantly as indicated in our zymography studies. Although it is difficult to speculate on the precise mechanisms responsible for increased TIMP-1 gene and protein expression in the BMVEC cells in which MMP-9 gene expression was silenced, we believe that it was the result of a consequent perturbation in the balance between the expression of MMP-9 and TIMP-1.

We did not observe any significant change in EMMPRIN expression in BMVEC transfected with QR-siRNA$^{\mathbf{MMP\text{-}9}}$. EMMPRIN stimulates MMP-9 in monocytes (Burggraf, 2005; Caudroy et al., 1999). Thus, the effect of MMP-9 gene knockdown on the expression of other genes is not indiscriminate and is highly specific. We are currently examining how these complicated inter-related pathways are regulated. The above findings are consistent with the premise that many genes involved in ECM remodeling also regulate the expression of each other. Further, based on the results of the TEER measurements across the in vitro BBB (Figure 11) we can speculate that MMP-9 is a key factor in the multiple mechanisms that may be involved in the breakdown of the BBB during neuroinflammatory processes and thus can be a major target for subsequent nanotherapy.

Nanoplexes provide an advantage over current therapeutic options, with respect to drug targeting, delivery and release, due to their ability to combine diagnosis and therapy. The goals of nanotherapy include improving the stability of nanoplexes in the biological environment; the capacity to mediate the biodistribution of active compounds; and the ability to load, transport, target, and release their therapeutic payloads. Although many previously described nanoparticles have been found to be cytotoxic, further research has led to better tolerated formulations as we describe herein. Subsequent clinical trials are necessary to assure that our nanoplex consisting of QDs and siRNA$^{\mathbf{MMP\text{-}9}}$ is both safe and effective for the therapy of neuroinflammatory disorders that disrupt the integrity of the BBB.

Albeit this manuscript describes a novel QR conjugated MMP-9 siRNA nanoplex that specifically targets MMP-9 gene expression in BMVECs that form the blood brain barrier, the present technology could be used to target the MMP-9 gene in various cell types such as leukocytes. This will help in modulating MMP-9 production under a variety of patho-physiological conditions. The current study, therefore, describes a general method for the knockdown of MMP-9 gene expression that could potentially have therapeutic application beyond the current area of investigation.

In conclusion this study supports the premise that MMP-9 plays a key role in BBB disruption during neuroinflammation, and that use of novel nanotechnology delivery system to silence MMP-9 expression in cells that constitute the BBB, may help preserve the integrity of the BBB and may be useful in clinical settings associated with BBB disruption.

MATERIAL AND METHODS

Nanoparticle formulation

Cadmium oxide (CdO), oleic acid, selenium (Se), trioctylphosphine (TOP), diethylzinc (Et_2Zn), hexamethyldisilathiane [(TMS)2S], chloroform, ammonium hydroxide, mono-N-(t-Boc)-propylenediamine, trifluoroacetic acid, lysine, mercaptosuccinic acid (MSA), mercaptoundecanoic acid (MUA) were purchased from Aldrich. All chemicals were freshly prepared for each new set of experiments. Semiconductor nanocrystals, quantum dots (CdSe/CdS/ZnS), are prepared by growing a CdS/ZnS graded shell on CdSe core in non-aqueous medium. Details of the preparation procedure are described in our previous publication (Qian et al., 2007). MSA was used to transfer the QDs from the non-aqueous phase to the aqueous phase, leading to the formation of water dispersible carboxyl-terminated QDs. In order to fabricate a net positive charge on the QD surface, the surface of the carboxyl-terminated QDs were further coated with a layer of the cationic, amine functionalized polymer poly (diallyldimethylammonium chloride (PDDAC) in two different QD:PDDAC ratios (represented as 15P and 30P, with the PDDAC amount twice in the later as compared to the former, for a fixed QD amount). The water dispersible, cationically modified QDs were then electostatically attached to the anionic siRNA molecules. The resultant nanoplexes (QD-siRNA) are prepared in fresh OptiMEM media (Invitrogen Corporation, Carlsbad, CA) before the start of each experiment.

Physical characterization of QD

The particle size of our nanoparticle formulations is determined by transmission electron microscopy (TEM). An aqueous dispersion of the nanoparticles is dried on formvar-coated copper grids obtained from Electron Microscopy Sciences Inc. and visualized using a JEOL JEM 2020 electron microscope. Simple spectrophotometry and spectrofluorimetry are used to study the spectral properties of the fluorescent nanomaterials. UV-Vis absorption spectra are recorded with a Shimadzu UV-3101 PC spectrophotometer using a quartz cuvette with a 1 cm path length. Fluorescence spectra are recorded on a Fluorolog-3 spectrofluorimeter (Jobin Yvon, Longjumeau, France).

Cell culture

Primary cultures of human brain microvascular endothelial cells (BMVEC) and normal human astrocytes (NHA) are obtained from Applied Cell Biology Research Institute (ACBRI) Kirkland, WA. Characterization of these cells demonstrated that >95% of BMVECs were positive for cytoplasmic VWF/Factor VIII and >99% of the NHA were positive for glial fribrillary acidic protein (GFAP). BMVEC are cultured in CS-C complete medium (ABCRI) with attachment factors (ABCRI) and Passage Reagent GroupTM (ABCRI). NHA are cultured in CS-C complete serum-free medium (ABCRI), supplemented with 10 μg/ml human epidermal growth factor (EGF), 10 mg/ml insulin, 25 μg/ml progesterone, 50 mg/ml transferrin, 50 mg/ml gentamicin, 50 μg/ml amphotericin, and 10% fetal bovine serum (FBS). Both BMVEC and NHA are obtained at passage 2 for each experiment and are used for all experimental paradigms between 2–8 passages, within 6 to 27 cumulative population doublings.

Cell viability assay

This assay measures the reduction of a tetrazolium component 3-(4,5-Dimethylthiazol-2-yl)-2,5-diphenyltetrazolium bromide (MTT) into an insoluble formazan product by the mitochondria of viable cells. The MTT assay is a quantitative and sensitive measure of cell proliferation, since it determines the growth rate of cells relative to a linear relationship between cell number and absorbance. Cells ($1X10^4$/ml) transfected with nanoplexes are incubated with

the MTT reagent for ~3 hr, followed by addition of a detergent solution to lyse the cells and solubilize the colored crystals. The samples are read in an ELISA plate reader at a wavelength of 570 nm. All the samples used are prepared in triplicate and values mean ± standard deviation are calculated.

Determination of the delivery of nanoplexes into BMVEC

Nanoplexes (QD-siRNA) are discrete spheres, having a mean size of 15–20 nm. They are sufficiently small to diffuse into cells by endocytosis and favor nucleic acid transfer and release from the endosome across the nuclear membrane. Nanoplex suspensions are prepared by adding 100 pmol siRNA$^{\mathbf{FAM}}$ (fluorescent silencer-Ambion) and 20 μL of QD nanoparticles (15P and 30P formulations) to 200 μL media without serum; they are incubated for 10 min at room temperature and added to 35 mm culture plates. Commercial transfection reagent (Xtreme, Roche Applied Biosystem) is used as a control to transfect 100 pmol siRNA$^{\mathbf{FAM}}$ into BMVEC according to the manufacturer's protocol. After 24 hr postransfection, the medium is replaced by fresh OptiMEM containing 10% FBS, and cells are cultured in an incubator (VWR Scientific, model 2400) at 37°C in a humidified atmosphere of 5% CO_2 in air. For confirming the consistency of the results, samples are prepared in triplicate. Fluorescence images are acquired after 24 hr with a spectral confocal microscope (TCSSP2, Leica Microsystems Semiconductor GmbH) with a HXC PL APO CS 63.0x1.40 oil immersion objective. The samples are excited by a laser at 488 nm (PDL800-D, PicoQuant GmbH). For siRNA$^{\mathbf{FAM}}$ detection, the photomultiplier tube (PMT) 1 is set with a filter of 520–540 nm for the detection of FAM to localize QDs, and PMT2 is set with a filter of 620–680 nm for the detection of QD bioconjugates. For QD-siRNA nanoplexes, PMT1 is set with a filter of 450–550 nm for autofluorescence, the PMT2 is set with a filter of 580–620 nm for QD (608 nm), and PMT3 is set with a filter of 640–690 nm QDs (608 nm). A water-immersion objective lens (Nikon, Fluor 60X, NA1.0) is used for the cells.

Real time, quantitative PCR (Q-PCR)

Total RNA is extracted from BMVEC using Trizol reagent according manufacturer's protocol, quantified by spectrophotometry (Nano-Drop ™ Wilmington, DE) and stored at −80°C until used. Q-PCR is used to quantitate MMP-9 and collagen IV expression in BMVEC cultures. Approximately $1x10^6$ BMVEC are harvested at 48 hr post transfection, and RNA is extracted as described above. The RNA is then reverse transcribed to cDNA using a reverse transcriptase kit (Promega Inc, Madison, WI). Relative abundance of each mRNA species is quantitated by Q-PCR using specific primers and the Brilliant® SYBR® green Q-PCR master mix (Stratagene Inc, La Jolla, CA). To provide precise quantification of the initial target in each PCR reaction, the amplification plot is examined and the data are interpreted as described (Bustin,2002; Radonić et al., 2004). Data are the mean ± SD of 3 separate experiments done in duplicate. Statistical significance was determined using ANOVA based on comparisons between QD-siRNA$^{\mathbf{MMP\text{-}9}}$ nanoplexes and the negative control.

Western blot analysis

Protein was extracted from transfected cells and untransfected controls using the M-PER® protein extraction reagent (Cat # 78503, Pierce, Inc, Rockford, IL). Immunodetection using standard "Western" blotting techniques as described in the Current Protocols in Immunology were used. 50 μg total protein extracted from cells was loaded per lane and separated by a 4–20% SDS-Tris glycine PAGE. Gels are blotted onto nitrocellulose membranes and membranes are probed with the Collgen Iα1, III, IV and V (Cat #'s sc-8788, sc-8781, sc-9302 and sc-9581 respectively from Santacruz Biotech; Santacruz CA) antibodies.

Measurement of MMP-9 and TIMP-1 protein expression using ELISA

Cell supernatants from transfected cells and untransfected controls were harvested 96 hrs post transfection and the levels of MMP-9 and TIMP-1 were measured in the supernatants using commercially available Quantikine®-colorimetric sandwich ELISAs kits [MMP-9 assay (Cat # DMP900) and TIMP-1 assay (Cat # DTM100)] from R & D systems, Minneapolis, MN. Briefly, the kit constitutes monoclonal antibody pre-coated microplates that are specific for MMP-9 or TIMP-1. Standards and samples are pipetted into the wells, followed by an incubation interval and then washing. An enzyme linked polyclonal antibody specific to the particular ligand is then added, followed by a washing step that ensures removal of unbound antibody enzyme reagent. A colorimetric detection is done using the stabilized chromogen TMB (tetramethybenzidine). The minimum detectable dose (MDD) dose of the MMP-9 assay was 0.156 ng/ml, and the standard curve ranged from 0–20 ng/ml. The minimum detectable dose (MDD) dose of the TIMP-1 assay was 0.08 ng/ml, and the standard curve ranged from 0–20 ng/ml. Data represented in Figure 8 are the mean ± SD from 4 separate experiments done in duplicate.

MMP zymography

Commercially prepared 4–16% zymogen gels containing gelatin and pre-stained with blue casein (Invitrogen Corporation, Carlsbad, CA) are used. M-PER® protein extraction reagent (Pierce, Inc, Rockford, IL) is used to extract the protein from approximately $1x10^6$ BMVEC. Typically, 30 μg protein isolated from untransfected and QD-siRNA$^{\mathbf{MMP\text{-}9}}$ transfected BMVEC is loaded on to the gel 48 hr post-transfection. Electrophoresis using a constant voltage of ~125V and a run time of 60–120 min in 1X Tris-glycine SDS running buffer is performed. The gel is incubated in Zymogram Renaturing Buffer (Invitrogen Corp., Carlsbad, CA), with gentle agitation for 30 min at room temperature, and then equilibrated in Zymogram Developing Buffer (Invitrogen Corporation, Carlsbad, CA) at 37°C for at least 4 hr. Areas of enzyme activity appear as clear bands against a dark blue background where the protease has digested the substrate. Appropriate molecular weight markers and a MMP-9 standard are also run in all gels to identify the band of interest. The band densities representing protease activity were determined by densitometry using Syngene software (Syngene Inc, Fedrick, MD). Data are the mean ± SD of 3 separate experiments done in duplicate. Statistical significance was determined using ANOVA based on comparisons between QD-siRNA$^{\mathbf{MMP\text{-}9}}$ nanoplexes and the negative control.

Immunofluorescent staining of BMVEC

Untransfected and transfected (control) BMVEC are grown to 70% confluence in a Petri dish with a glass bottom. Cells are fixed for 10 min at 37°C in 2% formaldehyde, followed by permabilization with ice-cold 90% methanol. Cells are then washed in 1X phosphate buffered saline (PBS) and treated with MMP-9 antibody. Standard immunofluoresecent staining procedures were followed. Imaging was performed with a confocal laser scanning microscope (TCS SP2 AOBS, Leica Microsystems Heidelberg GmbH) with a 63X oil immersion objective lens. A HeNe 633 nm laser was applied to excite the Alexa Fluor 647; an argon ion laser was applied to excite the dye DAPI.

In-vitro BBB model

The in-vitro BBB model used in this study utilizes 2-compartment, 6 well culture plates with the upper compartment separated from the lower by a 3 μ pore-size polyethylene terephthalate (PET) insert with a surface area = 4.67 cm^2 (Transwell plates, Costar). Untransfected and transfected BMVEC are cultured to confluence on the upper side of the PET insert, while a confluent layer of normal human astrocytes (NHAs) are grown on the underside (Persidsky, 1997). The transendothelial electrical resistance (TEER) across the in vitro BBB is used to

evaluate its functional integrity. TEER is measured with an ohm meter (Millicell ERS system, Millipore, Bedford, MA). Electrodes are sterilized using 95% alcohol and rinsed in sterile distilled water prior to measurement. Probes are positioned such that one end is immersed in media inside the upper filter chamber and the other is placed through the basolateral access hole into the media below. A constant distance of 0.6 cm is maintained between the electrodes at all times during TEER measurement. Formation of a functionally intact BBB with untreated BMVEC occurs by day 5–6 of culture and a value of ~250 Ω/cm^2 indicates an intact BBB.

Statistical Analysis

An Independent t- test or one-way ANOVA was applied to compare changes in different groups. Comparison among the means was performed with the post hoc Bonferroni analysis test using the PRISM 4 STATISTICAL SOFTWARE(GraphPad Software, Inc. La Jolla, CA) statistical analysis software. The quantitative data are presented as mean ± SD unless specified otherwise. Statistical significance was considered at $p < 0.05$.

Acknowledgements

This study was supported by grants from the National Institute of Health (RO1CA119397), the Kaleida Health Foundation, and the John R. Oishei Foundation. Support from the Center of Excellence in Bioinformatics and Life Sciences at the University at Buffalo is also acknowledged. The authors are also indebted to Dr. Kenneth M. Tramposch for providing his expert comments on this manuscript.

REFERENCES

Abbott N. Dynamics of CNS Barriers: Evolution, Differentiation, and Modulation. Cellular and Molecular Neurobiology 2005;25:5–23. [PubMed: 15962506]

Abbott NJ. Prediction of blood-brain barrier permeation in drug discovery from in vivo, in vitro and in silico models. Drug Discovery Today: Technologies 2004;1:407–416.

Annunziata P. Blood-brain barrier changes during invasion of the central nervous system by HIV-1. Journal of Neurology 2003;250:901–906. [PubMed: 12928906]

Asahi M, Sumii T, Fini ME, IItohara S, Lo EHC. Matrix metalloproteinase 2 gene knockout has no effect on acute brain injury after focal ischemia. Neuropharmacology And Neurotoxicology 2001;12:3003–3007.

Bergman MR, Cheng S, Honbo N, Piacentini L, Karliner JS, Lovett DH. A functional activating protein 1 (AP-1) site regulates matrix metalloproteinase 2 (MMP-2) transcription by cardiac cells through interactions with JunB-Fra1 and JunB-FosB heterodimers. Biochem J 2003 Feb 1;369(Pt 3):485–496. [PubMed: 12371906]

Bond M, Fabunmi RP, Baker AH, Newby AC. Synergistic upregulation of metalloproteinase-9 by growth factors and inflammatory cytokines: an absolute requirement for transcription factor NF-kappaB. FEBS Letters 1998;435:29–34. [PubMed: 9755853]

Brew K, Dinakarpandian D, Nagase H. Tissue inhibitors of metalloproteinases: evolution, structure and function. Biochim Biophys Acta 2000 Mar 7;1477(1–2):267–283. [PubMed: 10708863]

Burggraf D, Liebetrau M, Martens H, Wunderlich N, Jäger G, Dichgans M, Hamann GF. Matrix metalloproteinase induction by EMMPRIN in experimental focal cerebral ischemia. Eur J Neurosci 2005;22:273–277. [PubMed: 16029217]

Bustin SA. Quantification of mRNA using real-time reverse transcription PCR (RT-PCR): trends and problems. J Mol Endocrinol 2002;1:23–39. [PubMed: 12200227]

Caudroy S, Polette M, Tournier J-M, Burlet H, Toole B, Zucker S, Birembaut P. Expression of the Extracellular Matrix Metalloproteinase Inducer (EMMPRIN) and the Matrix Metalloproteinase-2 in Bronchopulmonary and Breast Lesions. J. Histochem. Cytochem 1999;47:1575–1580. [PubMed: 10567441]

Current Protocols in Immunology. Hoboken, NJ: John Wiley and Sons, Inc; 2007. Copyright © 2007 by

Ellis R, Langford D, Masliah E. HIV and antiretroviral therapy in the brain: neuronal injury and repair. Nat Rev Neurosci 2007;8:33–44. [PubMed: 17180161]

Foda HD, Zucker S. Matrix metalloproteinases in cancer invasion, metastasis and angiogenesis. Drug Discovery Today 2001;6:478–482. [PubMed: 11344033]

Gidday JM, Gasche YG, Copin JC, Shah AR, Perez RS, Shapiro SD, Chan PH, Park TS. Leukocyte-derived matrix metalloproteinase-9 mediates blood-brain barrier breakdown and is proinflammatory after transient focal cerebral ischemia. Am J Physiol Heart Circ Physiol 2005;289:H558–H568. [PubMed: 15764676]

Goldberg GI, Strongin A, Collier IE, Genrich LT, Marmer BL. Interaction of 92-kDa type IV collagenase with the tissue inhibitor of metalloproteinases prevents dimerization, complex formation with interstitial collagenase, and activation of the proenzyme with stromelysin. J Biol Chem 1992 Mar 5;267(7):4583–4591. [PubMed: 1311314]

Langford TD, Letendre SL, L GJ, Masliah E. Changing Patterns in the Neuropathogenesis of HIV During the HAART Era. Brain Pathology 2006;13:195–210. [PubMed: 12744473]

Li YY, McTiernan CF, Feldman AM. Interplay of matrix metalloproteinases, tissue inhibitors of metalloproteinases and their regulators in cardiac matrix remodeling. Cardiovasc Res 2000;46:214–224. [PubMed: 10773225]

Maquart FX, Pickart L, Laurent M, Gillery P, Monboisse JC, Borel JP. Stimulation of collagen synthesis in fibroblast cultures by the tripeptide-copper complex glycyl-L-histidyl-L-lysine-Cu2+ FEBS Lett 1988;238:343–346. [PubMed: 3169264]

Michalet X, Pinaud FF, Bentolila LA, Tsay JM, Doose S, Li JJ, Sundaresan G, Wu AM, Gambhir SS, Weiss S. Quantum Dots for Live Cells, in Vivo Imaging, and Diagnostics. Science 2005;307:538–544. [PubMed: 15681376]

Paul R, Lorenzl S, Koedel U, Sporer B, Vogel U, Frosch M, Pfister HW. Matrix metalloproteinases contribute to the blood-brain barrier disruption during bacterial meningitis. Ann-Neurol 1998;44:592–600. [PubMed: 9778257]

Persidsky Y, Gendelman HE. Development of laboratory and animal model systems for HIV-1 encephalitis and its associated dementia. J. Leukoc Biol 1997;62:100–106. [PubMed: 9226000]

Persidsky Y, Gendelman HE. Mononuclear phagocyte immunity and the neuropathogenesis of HIV-1 infection. Journal of Leukocyte Biology 2003;74:691–701. [PubMed: 14595004]

Persidsky Y, Stins M, Way D, Witte MH, Weinand M, Kim KS, Bock P, Gendelman HE, Fiala M. A model for monocyte migration through the blood-brain barrier during HIV-1 encephalitis. J Immuno 1997;158:3499–3510.

Prasad, PN. Introduction in Biophotonics. New York: Wiley; 2003.

Prasad, PN. Nanophotonics. New York: Wiley; 2004.

Pulliam L, Gascon R, Stubblebine M, McGuire D, McGrath MS. Unique monocyte subset in patients with AIDS dementia. Lancet 1997;349:692–695. [PubMed: 9078201]

Qian J, Yong K-T, Roy I, Ohulchanskyy TY, Bergey EJ, Lee HH, Tramposch KM, He S, Maitra A, Prasad PN. Imaging Pancreatic Cancer Using Surface-Functionalized Quantum Dots. The Journal of Physical Chemistry B 2007;111:6969–6972. [PubMed: 17552555]

Radonić A, Thulke S, Mackay IM, Landt O, Siegert W, Nitsche A. Guideline to reference gene selection for quantitative real-time PCR. Biochem Biophys Res Commun 2004;313:856–862. [PubMed: 14706621]

Lijnen HR, Van Hoef B, Lupu F, Moons L, Carmeliet P, Collen D. Function of the Plasminogen/Plasmin and Matrix Metalloproteinase Systems After Vascular Injury in Mice With Targeted Inactivation of Fibrinolytic System Genes. Arterioscler Thromb Vasc Biol 1998;18:1035–1045. [PubMed: 9672063]

Ramos-DeSimone N, Hahn-Dantona E, Sipley J, Nagase H, French DL, Quigley JP. Activation of Matrix Metalloproteinase-9 (MMP-9) via a Converging Plasmin/Stromelysin-1 Cascade Enhances Tumor Cell Invasion. J. Biol. Chem 1999;274:13066–13076. [PubMed: 10224058]

Schmidt R, Bultmann A, Fischel S, Gillitzer A, Cullen P, Walch A, Jost P, Ungerer M, Tolley ND, Lindemann S, Gawaz M, Schomig A, May AE. Extracellular Matrix Metalloproteinase Inducer (CD147) Is a Novel Receptor on Platelets, Activates Platelets, and Augments Nuclear Factor {kappa} B-Dependent Inflammation in Monocytes. Circ Res 2008;102:302–309. [PubMed: 18048771]

Schmidtmayerova H, Nuovo GJ, Bukrinsky M. Cell Proliferation Is Not Required for Productive HIV-1 Infection of Macrophages. Virology 1997;232:379–384. [PubMed: 9191852]

Sundstrom JB, Mosunjac M, Martinson DE, Bostik P, Donahoe RM, Gavanis AA. Effects of Norepinephrine, HIV Type 1 Infection, and Leukocyte Interactions with Endothelial Cells on the Expression of Matrix Metalloproteinases. Ansari. AIDS Research and Human Retroviruses 2001;17:1605–1614.

Teichberg VI. From the liver to the brain across the bloodâ€“brain barrier. Proceedings of the National Academy of Sciences 2007;104:7315–7316.

Timpl R, Wiedemann H, van Delden V, Furthmayr H, Kühn K. A network model for the organization of type IV of collagen molecules in basement membranes. Eur. J. Biochem 1981;12:203–211. [PubMed: 6274634]

Wang T, Zhang X, Li JJ. The role of NF-kappaB in the regulation of cell stress responses. Int Immunopharmacol 2002 Oct;2(11):1509–1520. [PubMed: 12433052]

Whitehead KA, Langer R, Anderson D. Knocking down barriers: advances in siRNA delivery. Nat Rev Drug Discov 2009;8:129–138. [PubMed: 19180106]

Woessner F Jr. Matrix Metalloproteinases and their inhibitors in connective tissue remodeling. FASEB J 1991;5:2145–2154. [PubMed: 1850705]

Wu DT, Woodman SE, Weiss JM, Mc MCM, D'Aversa TG, Hesselgesser J, Major EO, Nath A, Berman JW. Mechanisms of leukocyte trafficking into the CNS. J Neurovirol 2000:S82. [PubMed: 10871769]

Yong KT, Qian J, Roy I, Lee H, Bergey E, Tramposch K, He S, Swihart M, Maitra A, Prasad P. Quantum rod bioconjugates as targeted probes for confocal and two-photon fluorescence imaging of cancer cells. Nano Lett 2007;7:761–765. [PubMed: 17288490]

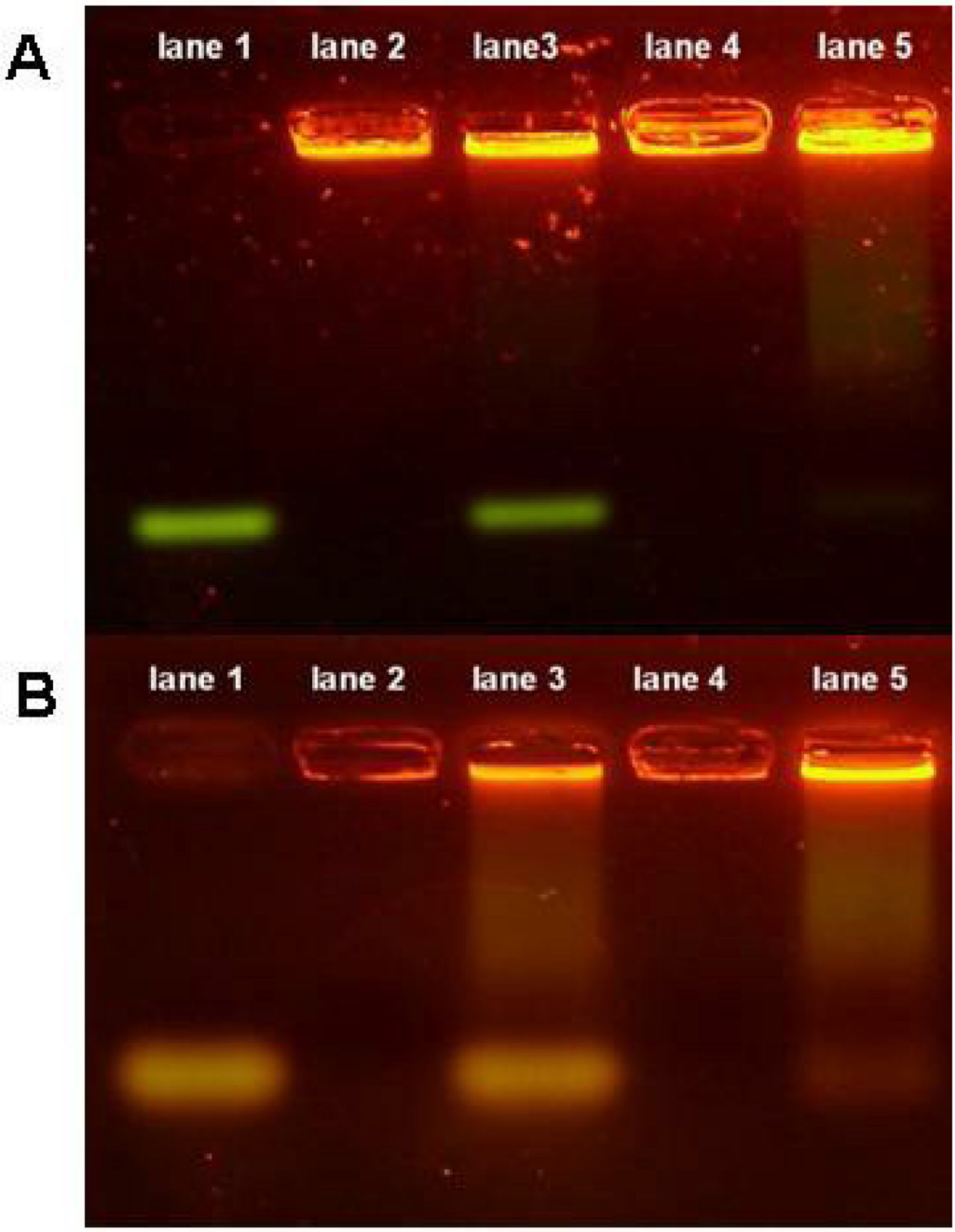

Figure 1. Effective binding of siRNA to QD as determined by agarose gel electrophoresis

A. Gel image with no ethidium bromide staining. lane 1: 50pmol free-siRNA$^{\mathbf{FAM}}$; lane 2: 15P QD; lane 3: QD-15P-siRNA$^{\mathbf{FAM}}$ nanoplex; lane 4: 30P QD; lane 5: QD-30P-siRNA$^{\mathbf{FAM}}$ nanoplex.

B. Ethidium bromide stained gel image. All lanes are identical to **A**, except that the siRNA used was not FAM labeled and was specific for MMP-9.

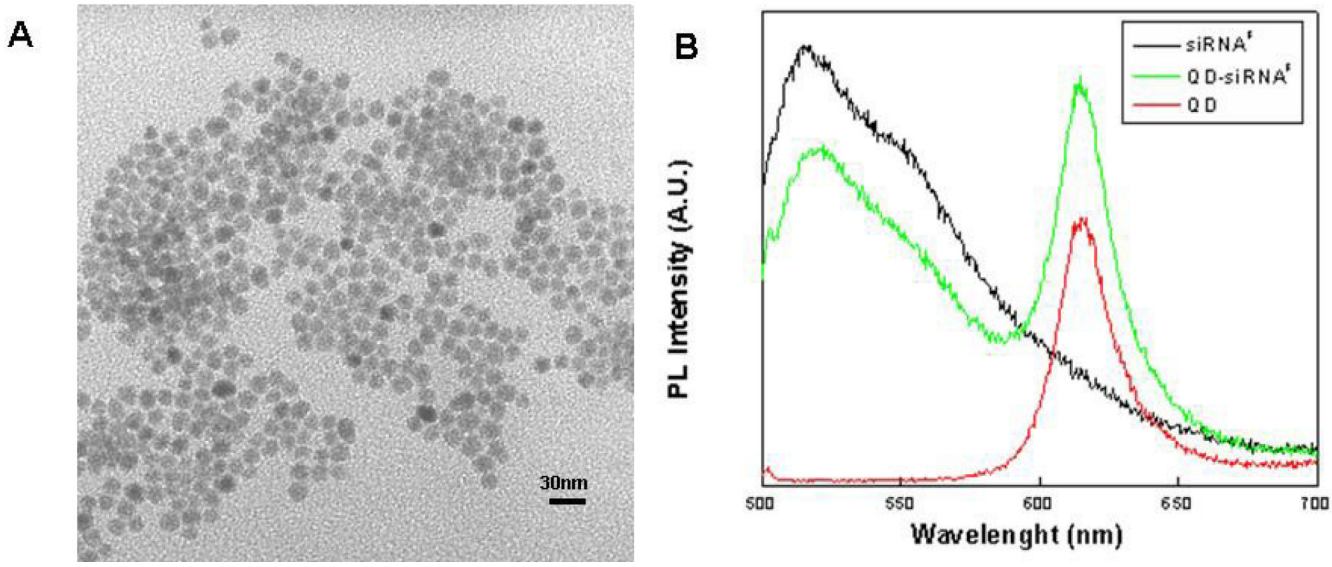

Figure 2. QD-siRNA^{FAM} nanoplex characterization

A. Transmission electron microscope image of nanoplexes showing that the average diameter of the nanoplex is 15 nm (bar scale = 30 nm). No aggregation was observed after nanoplex formation. **B**. Emission spectra of free siRNA^{FAM}, free QDs, and QD-siRNA^{FAM} nanoplexes.

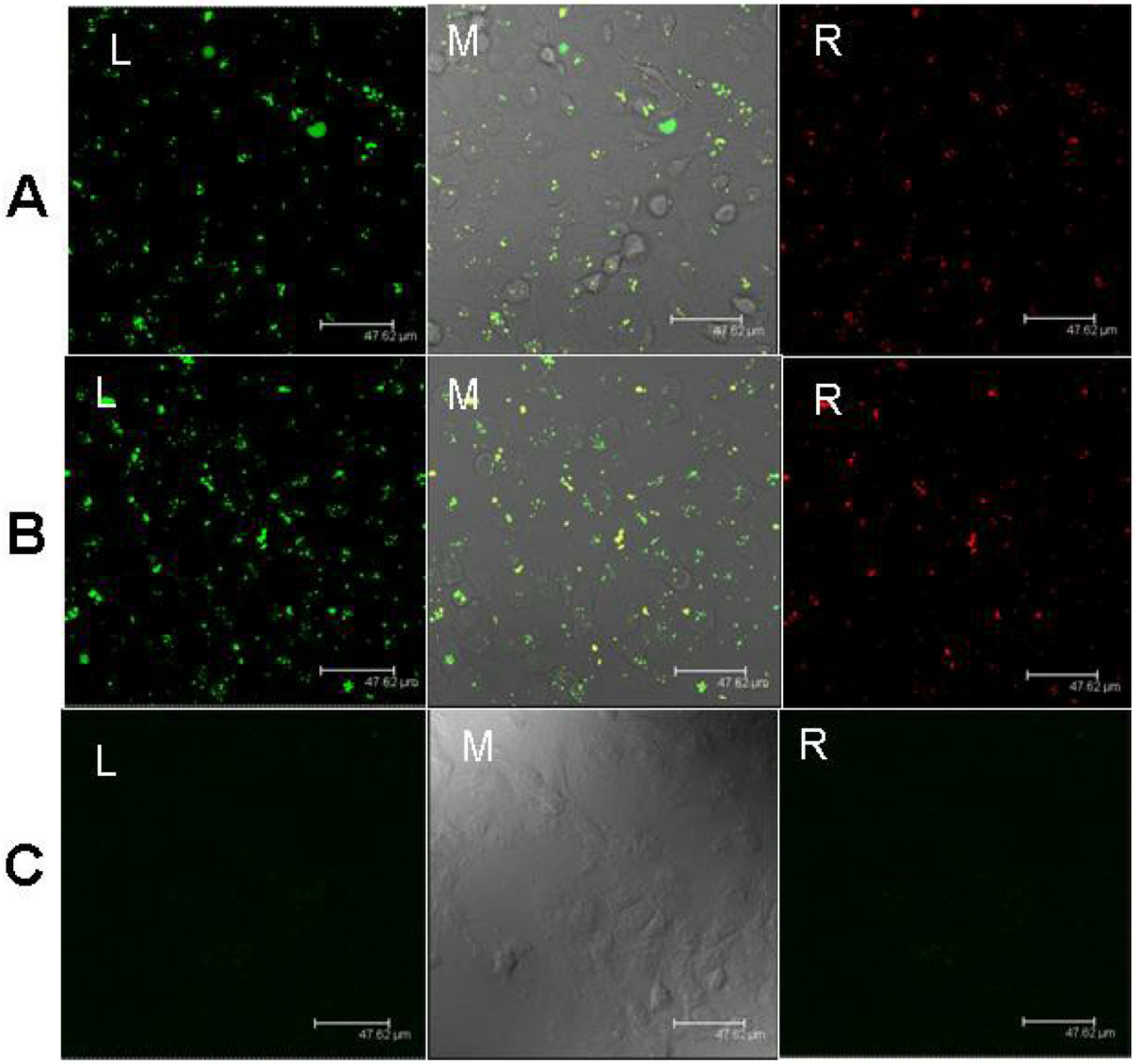

Figure 3. Confocal images of BMVEC treated with siRNA^{FAM} and QD-siRNA^{FAM} nanoplexes

BMVECs treated with (**A**) QD-15P-siRNA^{FAM}, (**B**) QD-30P-siRNA^{FAM}, and (**C**) free siRNA^{FAM}. Panel **L**: fluorescence (green) due to siRNA^{FAM}. Panel **M**: overlays of 2 fluorescence (QD and siRNA^{FAM}) and transmission images, and Panel **R**: fluorescence (red) due to QDs only.

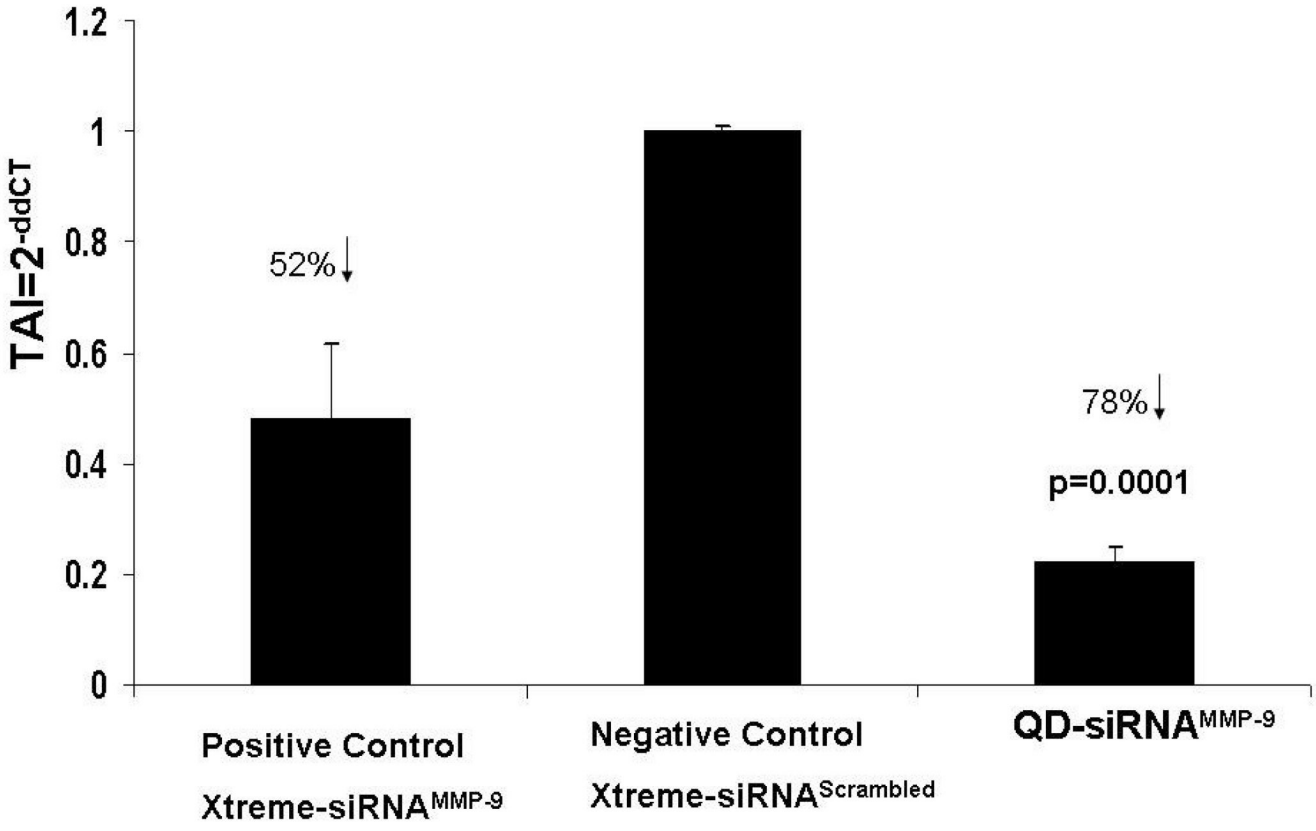

Figure 4. MMP-9 gene silencing in BMVEC by QD-siRNA^{MMP-9} nanoplexes

BMVECs were transfected with QD-siRNA^{MMP-9} or Xtreme-siRNA^{MMP-9} or Xtreme siRNA^{scrambled} for 48 hr. RNA was extracted, reverse transcribed, cDNA amplified and MMP-9 gene expression was determined by real time, quantitative PCR. Relative expression of mRNA species was calculated using the comparative C_T method. Data are the mean ± SD of 3 separate experiments done in duplicate. Statistical significance was determined using ANOVA based comparing QD-siRNA^{MMP-9} nanoplexes to the negative control samples.

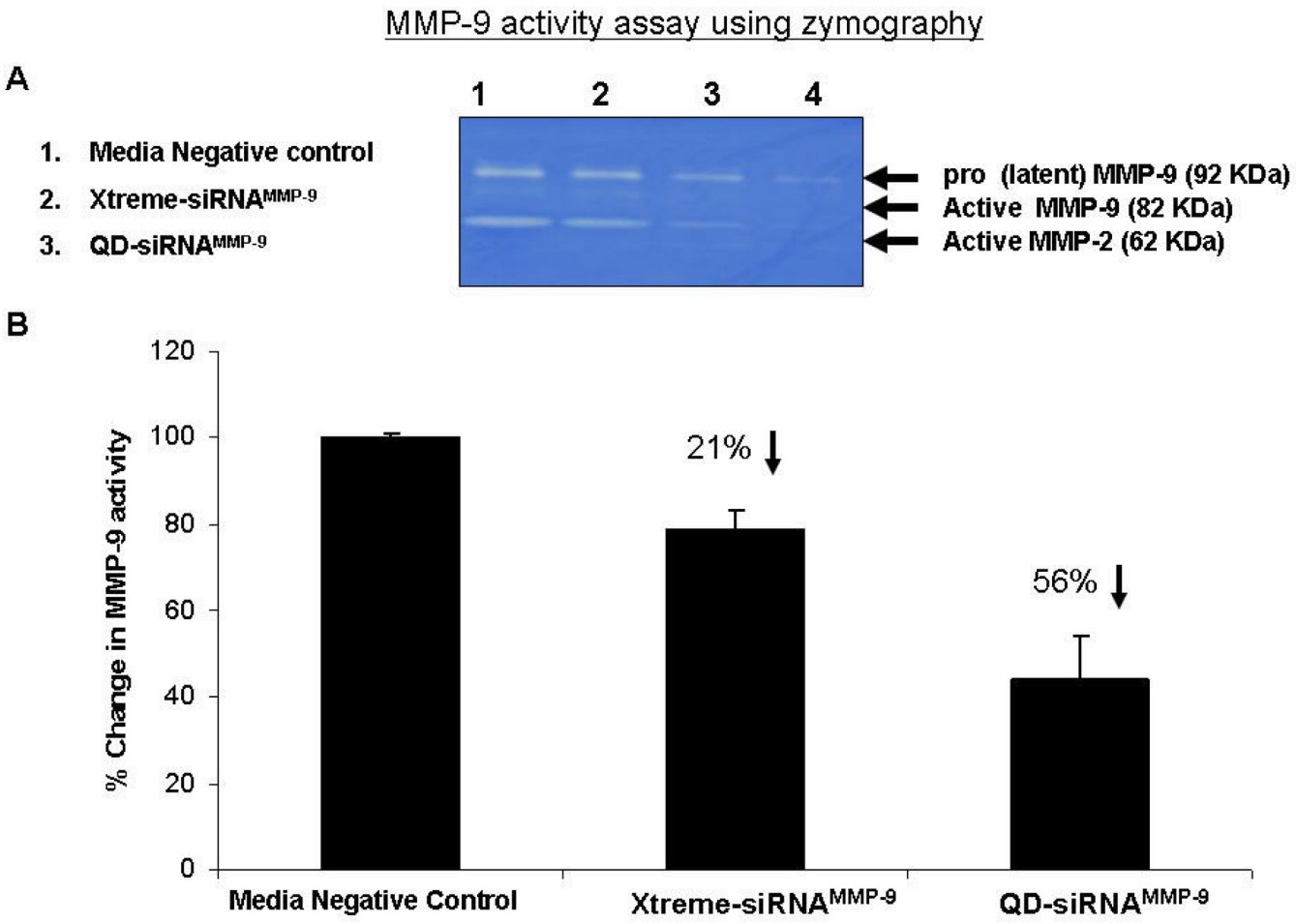

Figure 5. Effect of QD-siRNA^{MMP-9} nanoplexes on MMP-9 activity in BMVEC

BMVEC were treated in vitro with the QD-siRNA^{MMP-9} nanoplexes, positive (Xtreme-siRNA^{MMP-9}) transfection control and a negative media control for 48hr. Protein was isolated from the QD-siRNA^{MMP-9} transfected and untransfected BMVEC and MMP-9 actitivity was determined by zymography. Data are the mean ± SD of 3 separate experiments. Statistical significance was determined using ANOVA comparing the effects of QD-siRNA^{MMP-9} nanoplexes and the negative controls.

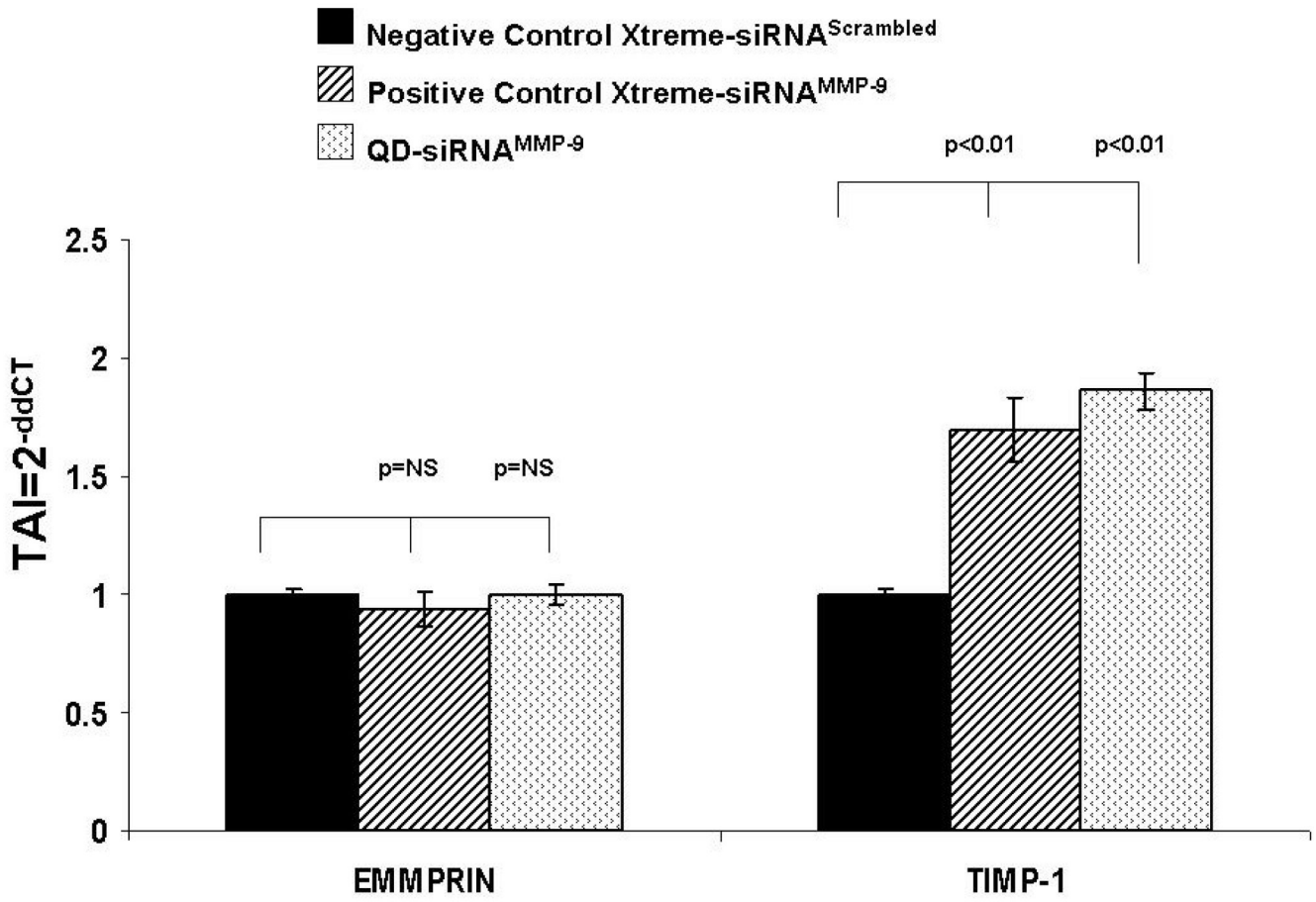

Figure 6. Effect of QD-siRNA^{MMP-9} nanoplexes on the expression of TIMP-1 and EMMPRIN genes in BMVEC

BMVEC were treated in vitro with either QD-siRNA^{MMP-9} nanoplexes, the positive transfection control (Xtreme-siRNA^{MMP-9}), or the negative transfection control (Xtreme-siRNA^{scrambled}) for 48 hrs. RNA was extracted, reverse transcribed, and the resultant cDNA was assayed for TIMP-1 and EMMPRIN gene expression by real time, quantitative PCR. Relative expression of mRNA species was calculated using the comparative C_T method. Data are the mean ± SD of 3 separate experiments done in duplicate. Statistical significance was determined using ANOVA based on comparison between the QD-siRNA^{MMP-9} nanoplexes, the positive transfection control and the negative control respectively.

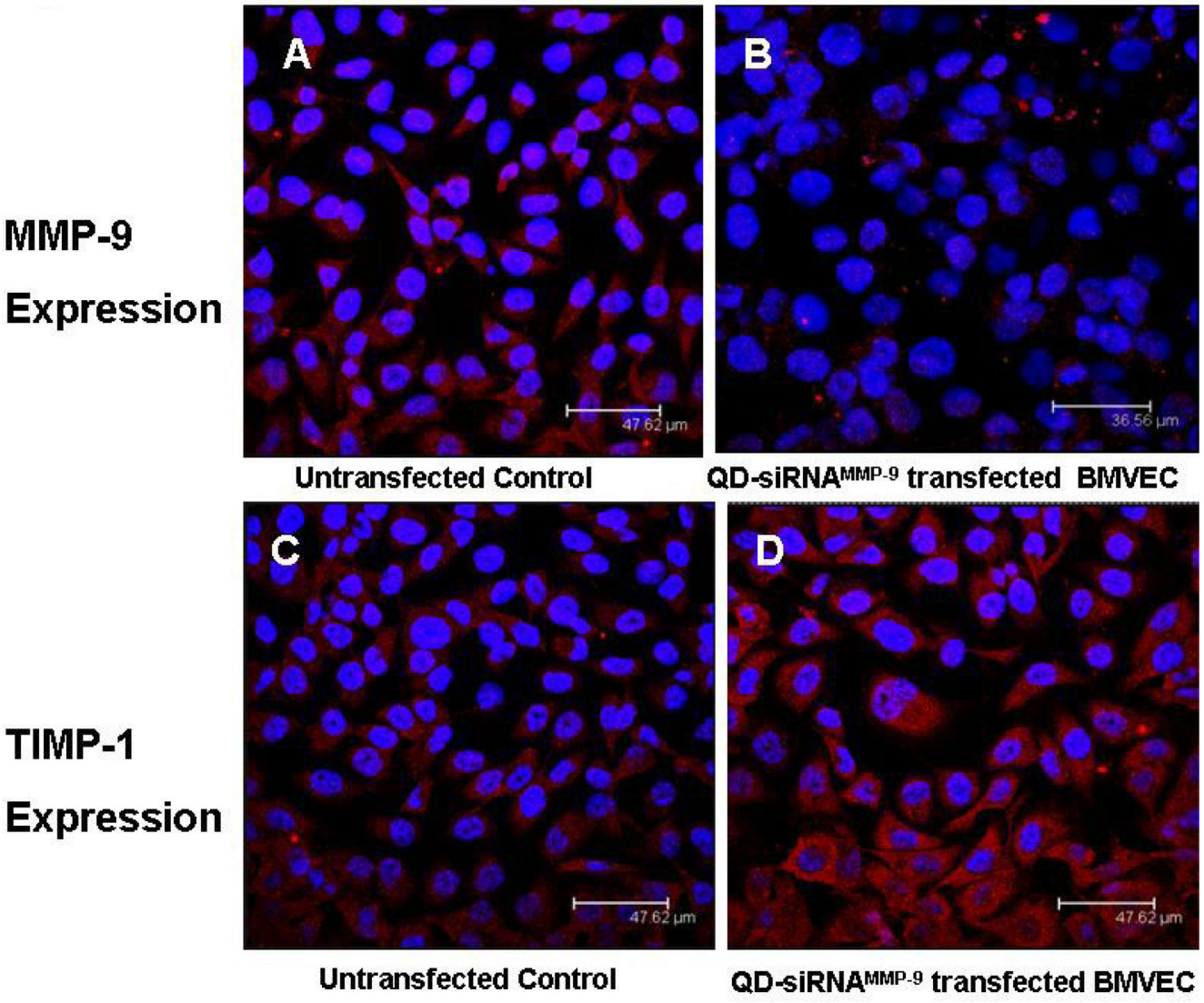

Figure 7. Immunofluorescent staining for MMP-9 and TIMP-1 in untransfected and QD-siRNA^{MMP-9} transfected BMVEC

A. MMP-9 expression in untransfected BMVEC. **B**. MMP-9 expression in QD-siRNA^{MMP-9} nanoplex transfected BMVEC. **C**. TIMP-1 expression in untransfected BMVEC; **D**. TIMP-1 expression in QD-siRNA^{MMP-9} nanoplex transfected BMVEC.

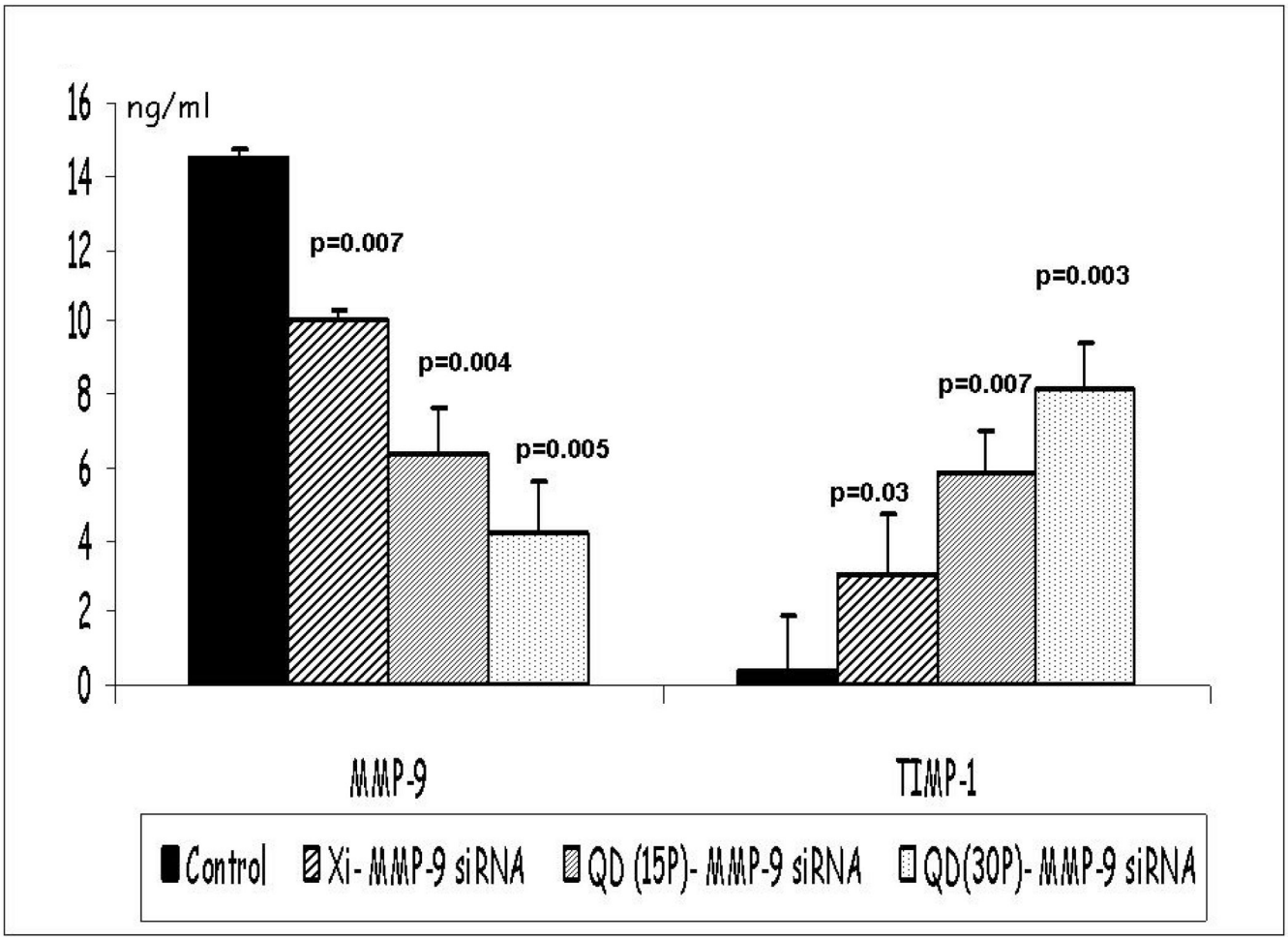

Figure 8. Effect of QD-siRNA^{MMP-9} nanoplexes on the protein expression of MMP-9 and TIMP-1 in transfected and untransfected BMVEC using ELISA

BMVEC were treated in vitro with 15P & 30P QD-siRNA^{MMP-9} nanoplexes, negative transfection control (Xtreme-siRNA^{scrambled}) and positive transfection control (Xtreme-siRNA^{MMP-9}) for 96 hrs. Cell supernatants were harvested and the levels of MMP-9 and TIMP-1 were measured in the supernatants using commercially available Quantikine®-colorimetric sandwich ELISAs kits [MMP-9 assay (Cat # DMP900) and TIMP-1 assay (Cat # DTM100)] from R & D systems, Minneapolis, MN. Data are the mean ± SD of 4 separate experiments done in duplicate. Statistical significance was determined using ANOVA based on comparisons between the transfected cells and the untransfected control.

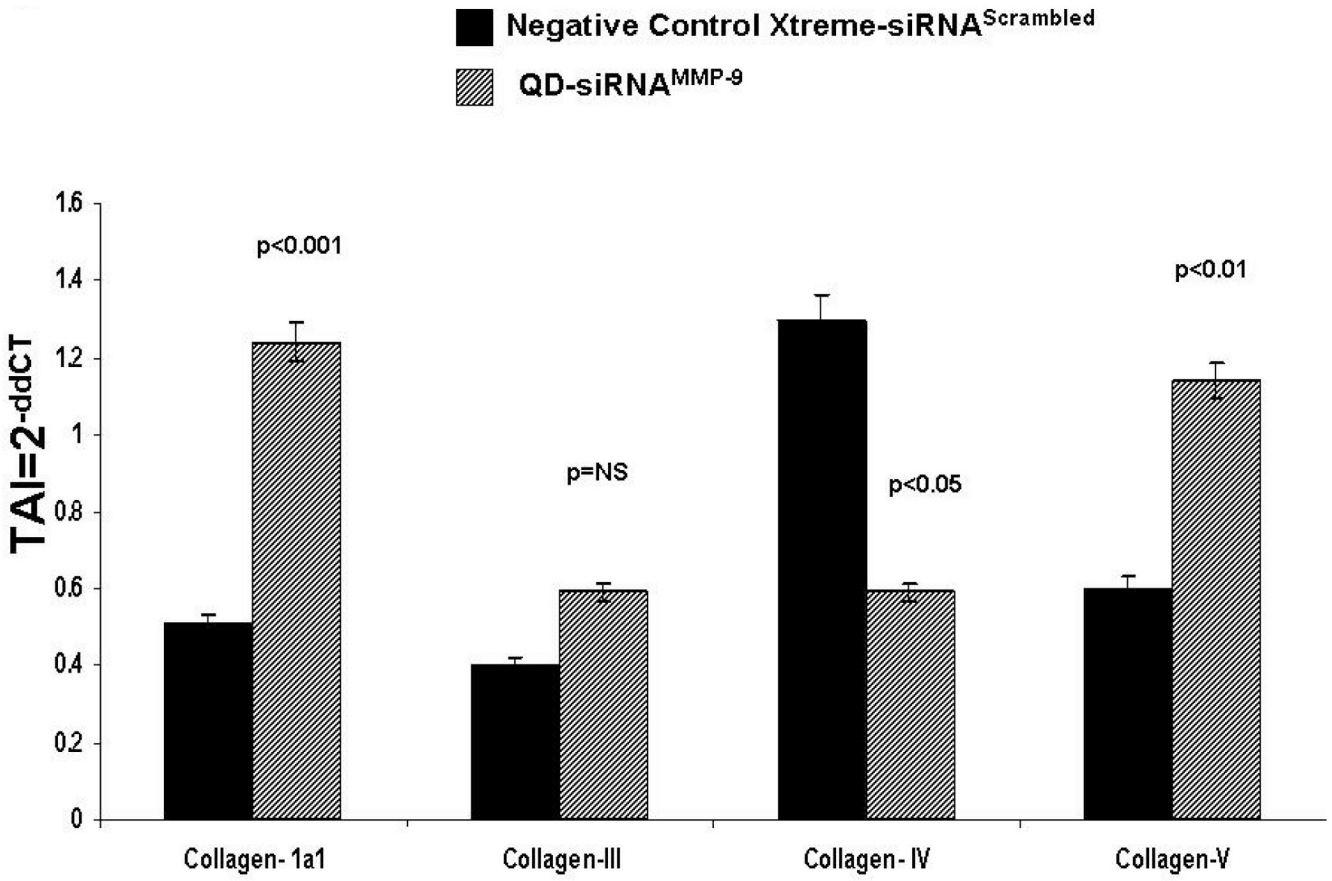

Figure 9. Modulation of collagen gene expression in BMVEC by QD-siRNA^{MMP-9} nanoplexes

BMVEC were treated in vitro with either QD-siRNA^{MMP-9} nanoplexes or the negative transfection control (Xtreme-siRNA^{scrambled}) for 48hrs. RNA was extracted, reverse transcribed, and the resultant cDNA was assayed for collagen 1α1, III, IV, and V gene expression by real time, quantitative PCR. Relative expression of mRNA species was calculated using the comparative C_T method. Data are the mean ± SD of 3 separate experiments done in duplicate. Statistical significance was determined using ANOVA based on comparisons between QD-siRNA^{MMP-9} nanoplexes and the negative control.

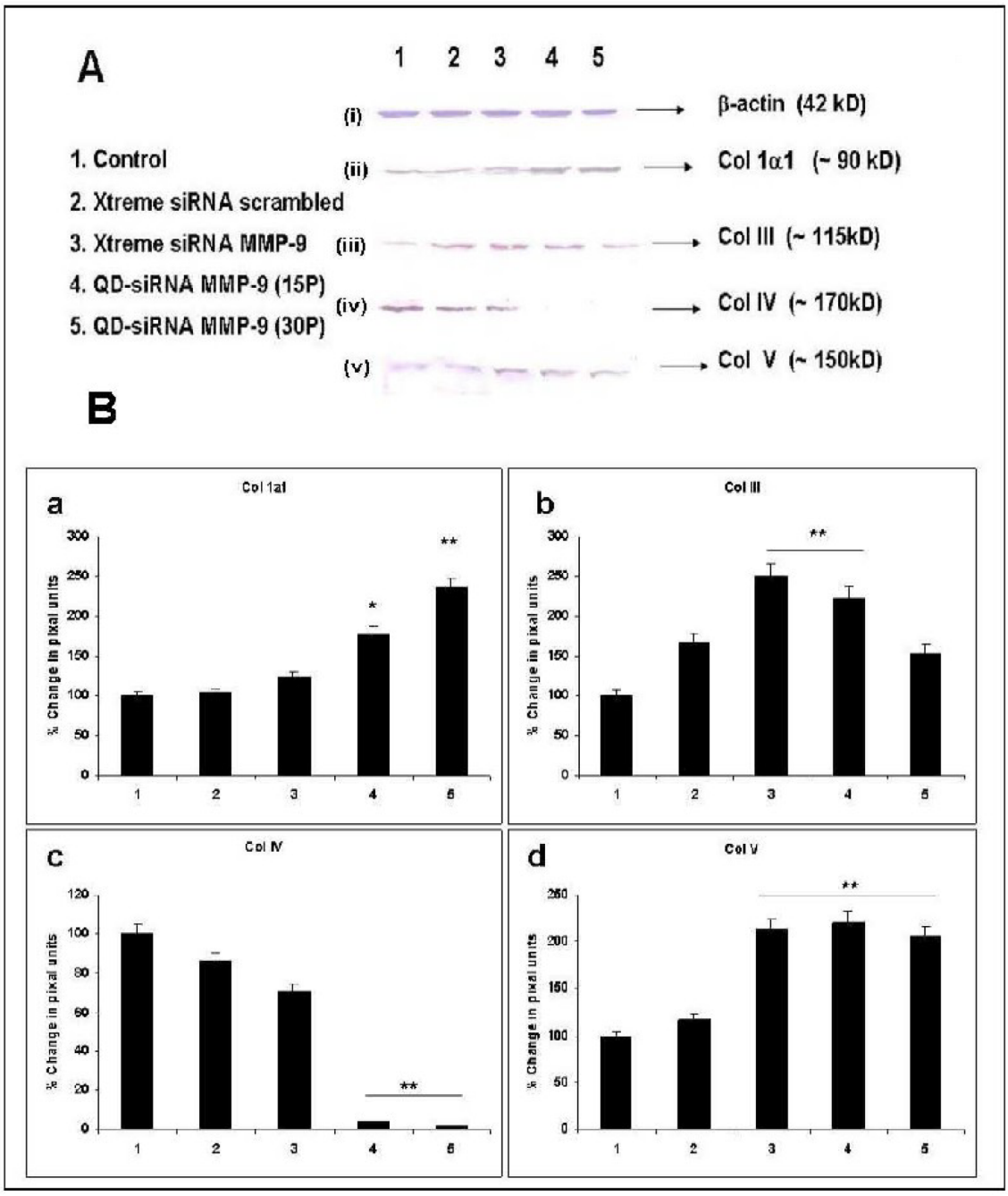

Figure 10. Effect of the QD-siRNA^{MMP-9} nanoplex on Collagen 1α1, III, IV and V protein expression in BMVEC cells

Western blot analysis of the lysates from transfected and untransfected BMVEC cells following their treatment in vitro with (15P)QD-siRNA^{MMP-9} nanoplexes (Lane 4); (30P) QD-siRNA^{MMP-9} nanoplexes (Lane 5), as well as both positive control (Xtreme-siRNA^{MMP-9}) (Lane 3) and negative control (Xtreme-siRNA^{scrambled}) (Lane 2), at 92 hrs post-transfection and comparisons made with an untransfected control (Lane 1). **Panel A** shows data from a representative western blot experiment showing (i) no change in b-actin (42 kDa band) protein expression, and (ii) a significant increase in Collagen 1α1 (~90 kDa band) protein expression, in cells treated with the 15P and 30P QD-siRNA^{MMP-9} nanoplexes (Lane 4 & 5), as opposed

to cells treated with untransfected control (Lane 1). (iii) a significant increase in Collagen III (~115 kDa band) protein expression, in cells treated with the 15P and 30P QD-siRNA$^{\mathbf{MMP\text{-}9}}$ nanoplexes (Lane 4 & 5), as opposed to cells treated with untransfected control (Lane 1). (iv) a significant decrease in Collagen IV (~170 kDa band) protein expression, in cells treated with the 15P and 30P QD-siRNA$^{\mathbf{MMP\text{-}9}}$ nanoplexes (Lane 4 & 5), as opposed to cells treated with untransfected control (Lane 1). (v) a significant increase in Collagen V (~150 kDa band) protein expression, in cells treated with the 15P and 30P QD-siRNA$^{\mathbf{MMP\text{-}9}}$ nanoplexes (Lane 4 & 5), as opposed to cells treated with untransfected control (Lane 1). **Panel B**: Graphical representation of the densitometric analysis of the all the protein bands showing percentage change in the protein expression for a)Collagen 1α1; b) Collagen III; c) Collagen IV and d) Collagen V respectively in transfected cells as compared to the untransfected controls. Data shown are mean ± SD of results from 3 separate experiments, and statistical significance was determined using ANOVA.

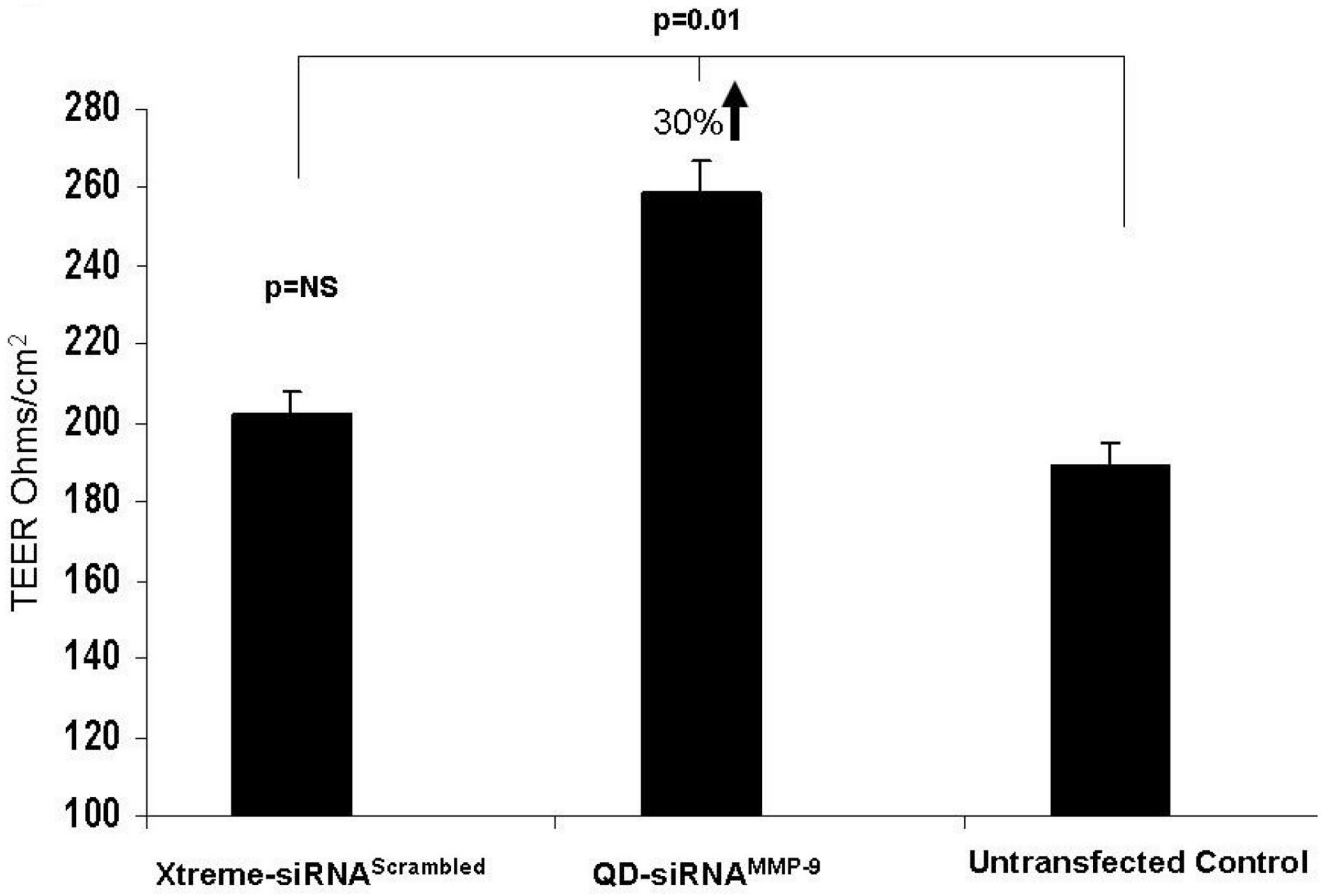

Figure 11. MMP-9 gene silencing by QD-siRNA^{MMP-9} nanoplexes affects the functional integrity of an in-vitro BBB model

BMVEC, untransfected or transfected with QD-siRNA^{MMP-9} nanoplexes, were used to form a model BBB in vitro. The transendothelial electrical resistance (TEER) was measured 48 hr post-transfection. Using QD-siRNA^{MMP-9} transfected BMVEC to form the BBB resulted in significantly higher TEER values compared to untransfected or QD-siRNA^{scrambled} negative controls. Data shown are the mean ± SD of 3 separate experiments. Statistical significance was determined using ANOVA based on comparisons between transfected cells and controls.